Quasi-static Analysis of Shielded Multiconductor Transmission Lines for Triple Modal Reservation

Evgeniya Chernikova
Television and Control Department
Tomsk State University of Control Systems and Radioelectronics
Tomsk, Russian Federation
chiernikova96@mail.ru

Anton Belousov
Television and Control Department
Tomsk State University of Control Systems and Radioelectronics
Tomsk, Russian Federation
ant1lafleur@gmail.com

2021 IEEE Ural Symposium on Biomedical Engineering, Radioelectronics and Information Technology (USBEREIT) | 978-1-7281-7691-8/21/$31.00 ©2021 IEEE | DOI: 10.1109/USBEREIT51232.2021.9455008

***Abstract*—The paper analyzes two structures of multiconductor transmission lines (MCTL) for triple modal reservation of critical circuits in radio-electronic equipment. The MCTLs with the reference conductor around, and above and below were considered. A computational experiment for these MCTLs was performed. In the range of parameters, time responses to various excitation types and frequency responses under the control of the useful signal bandwidth were obtained. The effect of changing the cross section parameters of the MCTL on the values of the maximum output voltage and bandwidth was estimated. By means of parametric optimization of the MCTL, it became possible to achieve equalization of the time intervals between the decomposition pulses and an increase in the attenuation of the output voltage from 0.5 V to 0.29 V and from 0.25 V to 0.24 V for the MCTL with the reference conductor around, and above and below, respectively. The analysis of the results showed the admissibility of using these MCTLs as devices for triple modal reservation.**

Keywords—electromagnetic compatibility, cold reservation, pulse signal, modal reservation, multiconductor transmission lines

I. Introduction

Radio-electronic devices (RED) are widely used in almost every industry of the modern world. With the increase of complexity and availability of REDs, the problem of ensuring their electromagnetic compatibility (EMC) becomes more relevant. It is especially important to ensure the proper level of reliability of vulnerable and strategically important facilities, for example, telecommunication networks, banking systems, government buildings, nuclear power plants, military bases, onboard equipment, etc. [1, 2]. The problem of ensuring the reliability of complex and critical REDs is traditionally solved by means of reservation [3]. Reservation increases the survivability of the entire system and is one of the most effective means of reducing damage from various circuit failures. In addition, in many cases the need for reservation is dictated by industrial safety requirements or government regulations and standards.

One of the widely used reservation types is cold reservation. Its principle is based on the fact that if a functioning (reserved) circuit fails, power is supplied to the passive (reserving) circuit. Meanwhile, reservation devices increase the mass, size and cost of the RED. At the same time, the increasingly aggravating problem of EMC ensurance requires the adoption of additional measures to protect electronic equipment, for example, from the excitation of powerful ultrashort pulses (USP) [4, 5]. Modal filtration technology is used to protect against USPs [6]. Its key point lies in minimizing the maximum output voltage (U_{max}) of an interference pulse in a multiconductor transmission line (MCTL) by decomposing it into a sequence of pulses of lower voltages due to the difference in the velocities of modes propagating in the MCTL.

To solve the problem of providing interference protection and increasing the level of reliability, a method of circuit modal reservation (MR) has been proposed [7]. MR means the combination of modal filtration effect as well as the cold reservation [8, 9]. To ensure higher reliability, a method of triple MR of interconnections (1 reserved and 3 reserving) has been proposed [10]. However, existing studies of triple MR are not enough to objectively assess its use. Meanwhile, it is relevant to consider various configurations of the MCTL suitable for triple MR. For this, in this work, we propose to perform preliminary simulation and analysis of new interference suppressing MCTLs with triple MR: with the reference conductor around, and above and below. The purpose of the work is to carry out such research.

II. Simulation Approaches

The cross-sections of the investigated MCTLs with the reference conductor around, and above and below are shown in Fig. 1a, b. The MCTL with the reference conductor around is a shielded cable similar in cross-section to flat flexible cable (employed for switching lighting devices and connecting low-power devices) and power cable of PVC-insulated conductor (used in industrial premises, at power plants, in distribution and lighting devices, etc.). Cross-section parameters are: the conductor radius r_c=1.5 mm, the dielectric radius r_d=1.75 mm, the reference conductor radius r_r=4.35 mm and the relative dielectric permittivity ε_r=10. The MCTL with the reference conductor above and below is a shielded strip structure in which the broad-side coupling provides high values of both the attenuation of the exciting USP and the differences in per-unit-length mode delays ($\Delta\tau$). Cross section parameters are: the width of the conductors w=1600 μm, the separation between them s=510 μm, the thickness of the conductors t=35 μm, the thickness of the dielectric h=500 μm, ε_r=4.5.

The simulation was carried out using a quasi-static approach implemented in the TALGAT 2019 software [11], which allows for the following for circuits with MR:

- Construction of the cross-section geometric models of the MCTL.
- Calculation of the matrices of per-unit-length coefficients of electrostatic (**C**) and electromagnetic (**L**) inductances, as well as per-unit-length resistances (**R**) and conductances (**G**).

The reported study was funded by Russian Science Foundation (project №20-19-00446) in TUSUR.

- Calculation of time and frequency responses in a range of parameters to evaluate the MCTL characteristics.

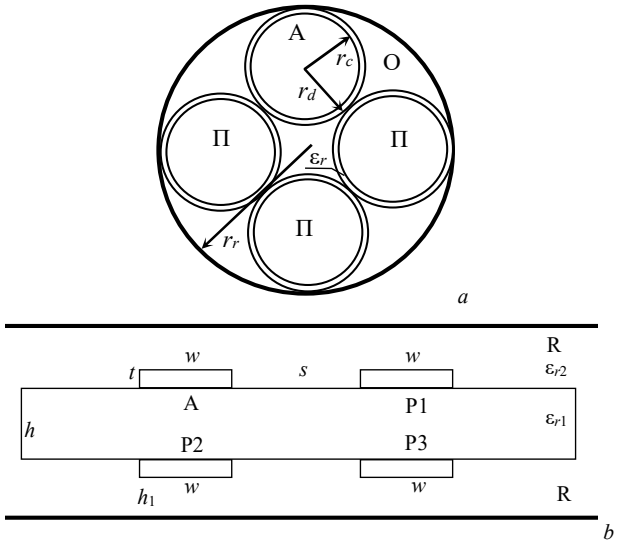

Fig. 1. Cross-section of the MCTL with the reference conductor around (*a*) and above and below (*b*), where conductors: A is active; P is passive; R is reference.

Fig. 2*a* shows the equivalent circuit of the MCTLs in general form. The length of the MCTLs (*l*) is equal to 1 m, and the *R* values were chosen from the condition of MCTL matching with the path [12]. To simulate the time response, three sources of excitation were selected: trapezoidal pulse (Fig. 2*b*), electrostatic discharge (ESD) (Fig. 2*c*) and digitized signal of a real USP generator (Fig. 2*d*). When a trapezoidal pulse was applied, an EMF source with an amplitude of 2 V was used with rise, fall, and flat top durations of 50 ps each, so that the total duration was 150 ps. The ESD pulse has a current waveform close to the third degree of severity with values τ_1=1.56 ns, τ_2=3.87 ns, τ_3=7.77 ns, τ_4=270 ns, I_1=18.56 A, I_2=10.12 A, n=3 according to IEC 61000-4-2. The waveform of the real USP generator is represented by a digitized signal of oscilloscope computational combined C9-11 with an amplitude of 0.249 V and the rise duration of 312 ps, fall of 259 ps and flat top of 8 ps (by 0.1–0.9 levels) and the total pulse duration (by 0.5 level) of 257 ps. Simulation of the frequency response of the MCTL was performed under the harmonic excitation of an EMF source of 2 V in the frequency range from 1 MHz to 3 GHz. Optimization was performed using heuristic search [13].

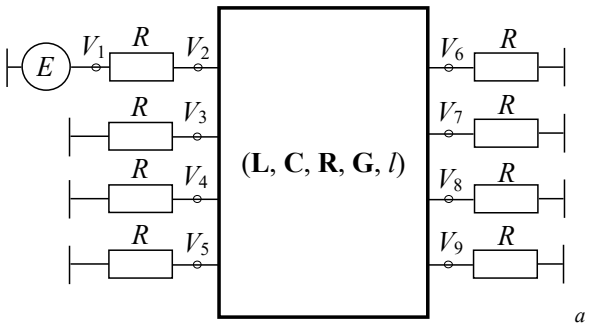

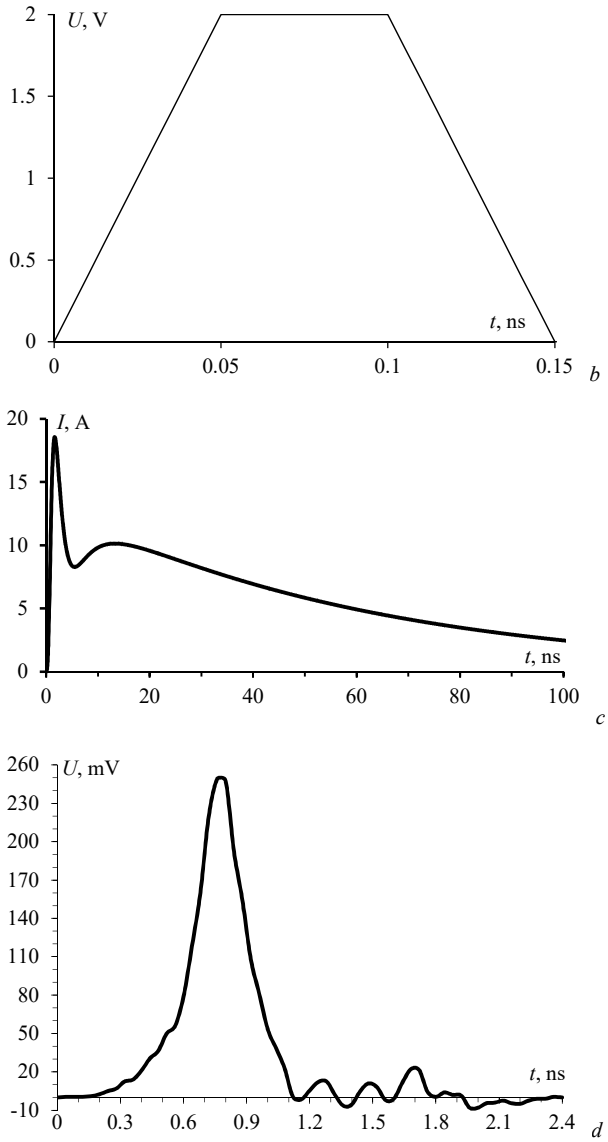

Fig. 2. Equivalent circuit of the considered MCTLs (*a*) and waveforms of the exciting trapezoidal pulse signal (*b*), ESD current (*c*) and a digitized real USP signal (*d*).

III. Computational Experiment

A. Time domain

Simulation of the time responses was performed in the range of the cross-section parameters with a small deviation of their values relative to parameter set 1. For MCTL with the reference conductor around the parameter set was the following:

1. r_c=1.5 mm, r_d=1.75 mm, r_r=4.35 mm.
2. r_c=2 mm, r_d=2.25 mm, r_r=5.5 mm.
3. r_c=1 mm, r_d=1.25 mm, r_r=3.1 mm.

For MCTL with the reference conductor above and below the parameter set was the following:

1. s=510 μm, w=1600 μm, t=35 μm, h=500 μm.
2. s=550 μm, w=1650 μm, t=70 μm, h=550 μm.
3. s=450 μm, w=1550 μm, t=18 μm, h=450 μm.

Voltage waveforms at the output of the MCTLs are shown in Fig. 3. Table 1 summarizes the U_{max} values and the per-unit-length mode delays (τ_i). From the simulation results for the MCTL with the reference conductor around, it can be seen that, in addition to the superposition of pulses 1 and 2, the difference in the cross-section parameter values (sets 2 and 3) from the average affects the τ_i values, and the maximum difference between adjacent τ_i values when changing the parameter values observed at pulse 3 (far right) and is 2.435 ns/m. Thus, the maximum deviations of the τ_i values are 0.31 ns/m for pulses 1 and 2 (which arrived at the same time), 0.24 ns/m for pulse 3, and 2.435 ns/m for pulse 4.

From the simulation results for the MCTL with the reference conductor above and below, it can be seen that the difference in the cross-section parameter values (sets 2 and 3) from the average has the least effect on the τ_3 value, and the maximum difference between adjacent values is observed for τ_1 and is 0.275 ns/m. So, if the parameter values are deviated, the maximum deviation of τ_i values for pulse 1 at the output is 0.275 ns/m, for pulse 2 – 0.215 ns/m, for pulse 3 – 0.165 ns/m, and for pulse 4 – 0.215 ns/m. Nevertheless, when the parameter values deviate from the average for both MCTLs, the U_{max} value practically does not change. The maximum attenuation of the exciting USP for the MCTL with the reference conductor around is 2.01 times. This is due to the superposition of pulses 1 and 2 because of the same electromagnetic coupling between active and passive conductors. In this case, the MCTL with the reference conductor above and below can provide an attenuation of 3.98 times relative to the input voltage.

Further, we consider the cases when an ESD and a digitized real USP signal are excitations for the same MCTLs. When simulating the time response to the excitation of the ESD and the digitized signal, a parameter set 1 is chosen.

In the case of the ESD extation, only its peak «burst» of about 4 ns duration undergoes modal decomposition (however, due to the long duration, it is impossible to observe total ESD decomposition). The maximum current amplitudes are equal to 10,36 A and 9,22 A for each MCTL, respectively. Fig. 4 shows the current waveforms at the output of the MCTLs. It can be seen that the shape of the current at the output remained practically unchanged. Nevertheless, the output amplitude values of the considered MCTLs decreased by 1.9 A for the MCTL with the reference conductor around, and by 1.32 A for the MCTL with the reference conductor above and below compared to the input amplitude and were equal to 8.46 A and 7.9 A, respectively. Obviously, due to the incomplete matching of the MCTL with the path, multiple reflections are present, which distort the original waveform of the ESD current.

Simulation of the MCTL under the excitation of a digitized signal of the real USP was performed taking into account the losses in the conductors and dielectric. The output voltage waveforms when the MCTL was excited by a digitized signal are shown in Fig. 5. Since the total duration of the exciting USP is longer than the maximum value of the difference of the per-unit-length delays ($\Delta\tau$), there is a partial overlapping of decomposition pulses, due to which it is impossible to estimate the τ_i values. Nevertheless, it is possible to estimate the value of U_{max}, and the attenuation factor for the MCTLs with the reference conductor around, and above and below, which are 0.109 V and 0.047 V, and 2.28 times and 5.29 times (relative to the input voltage), respectively.

B. Frequency domain

The frequency responses of the MCTL with reference conductor around and above and below were obtained similarly to time response simulations and are presented in Fig. 6. The bandwidths at minus 3 dB (Δf) and first resonance frequencies (f_1) are summarized in Table 1. From the simulation results, it can be seen that Δf for the MCTL with the reference conductor around differs in all parameter sets (the deviation between parameters sets 1 and 2 is 0.2394 GHz, between sets 2 and 3 – 0.179 GHz, and between sets 2 and 3 – 0.06 GHz). The f_1 value for different parameter sets also differs from each other (the maximum deviation is 0.437 GHz between parameter sets 1 and 2). The Δf values for the MCTL with the reference conductor above and below is different from parameter sets 2 relative to the rest (the deviation is about 0.013 GHz). The f_1 value is also slightly different for each parameter set (the maximum deviation is 0.118 GHz between parameter sets 1 and 2).

IV. Parametric Optimization

When optimizing the MCTL with the reference conductor around, r_i varied in the range of 200–4000 μm. As a result of optimization, the following parameters were obtained: r_c=900 μm (conductor A); r_c=800 μm (conductor P2); r_c=700 μm (conductor P3); r_c=800 μm (conductor P1); r_d=970 μm (dielectric around A); r_d=950 μm (dielectric around P2); r_d=950 μm (dielectric around P3); r_d=950 μm (dielectric around P1); r_r=3500 μm; ε_r=30 (dielectric around A); ε_r=16 (dielectric around P2); ε_r=6 (dielectric around P3); ε_r=5 (dielectric around P1). Note that it is much more difficult to achieve complete decomposition of the exciting USP in the MCTL with the reference conductor around (with a circular cross-section) than in strip structures. This is due to the initially identical electromagnetic couplings between active and passive conductors. Nevertheless, after optimization, the U_{max} value was 0.29 V (before optimization it was 0.5 V). An increase in the attenuation of the exciting USP was obtained because different couplings between conductors A-P1 and A-P3 were established. The voltage waveform at the MCTL output after optimization is shown in Fig. 7*a*.

When optimizing the MCTL with the reference conductor above and below, the values of *s* and *w* varied in the range of 50–2000 μm; *t* – in the range of 18–175 μm and *h* – in the range of 200–3000 μm. As a result of optimization, the following parameters were obtained: *s*=200 μm (not changed); *w*=260 μm; *t*=135 μm and *h*=100 μm. After optimization the U_{max} value was 0.24 V (before optimization it was 0.25 V). As a result of optimization, it was possible, first of all, to equalize the time intervals between the decomposition pulses so that $\Delta\tau$ is 0.68, 0.71, and 0.72 ns/m. The voltage waveform at the MCTL output after optimization is shown in Fig. 7*b*.

TABLE I. RESULTS OF CALCULATING THE TIME AND FREQUENCY RESPONSES

Structure with a reference conductor	Parameter sets	Parameters						
		U_{max}, V	τ_1, ns/m	τ_2, ns/m	τ_3, ns/m	τ_4, ns/m	Δf, GHz	f_1, GHz
Around	1	0.497	5.475	5.475	5.78	6.37	0.337	1.666
	2	0.498	5.695	5.695	5.925	8.805	0.098	2.103
	3	0.496	5.785	5.785	6.02	7.7	0.158	1.861
Above and below	1	0.249	7.16	8.37	8.86	9.17	0.17	0.798
	2	0.247	7.4	8.245	8.755	9.055	0.183	0.916
	3	0.251	7.435	8.46	8.92	9.27	0.172	0.846

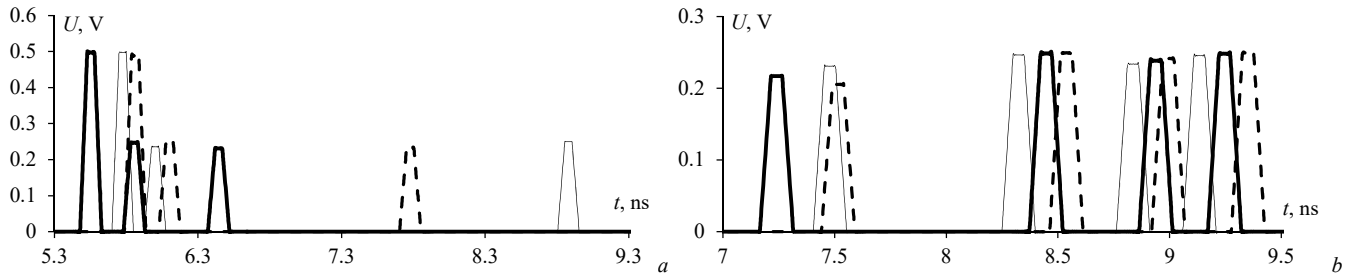

Fig. 3. Voltage waveforms at the MCTL output with the reference conductor around (*a*) and above and below (*b*) at parameter sets 1 (——), 2 (—) and 3 (– –).

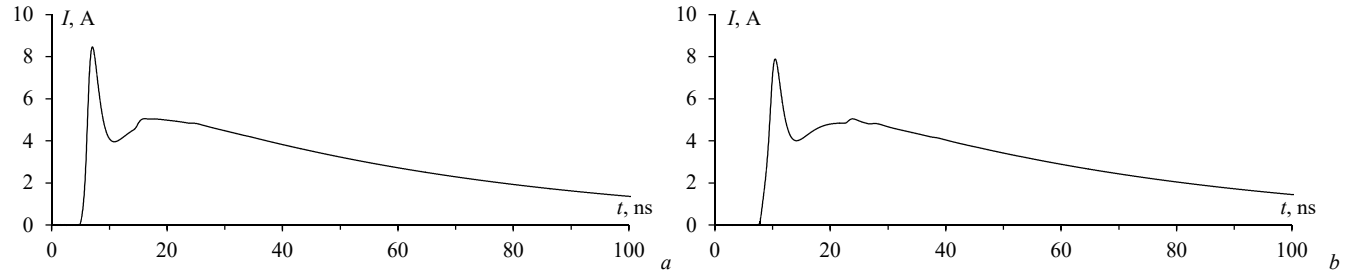

Fig. 4. Current waveforms at the MCTL output with the reference conductor around (*a*) and above and below (*b*) when excited by ESD.

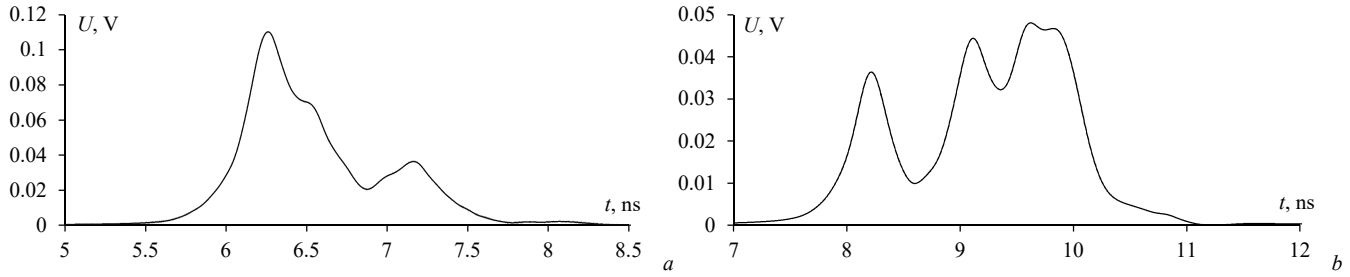

Fig. 5. Voltage waveforms at the MCTL output with the reference conductor around (*a*) and above and below (*b*) when excited by a signal from the USP generator.

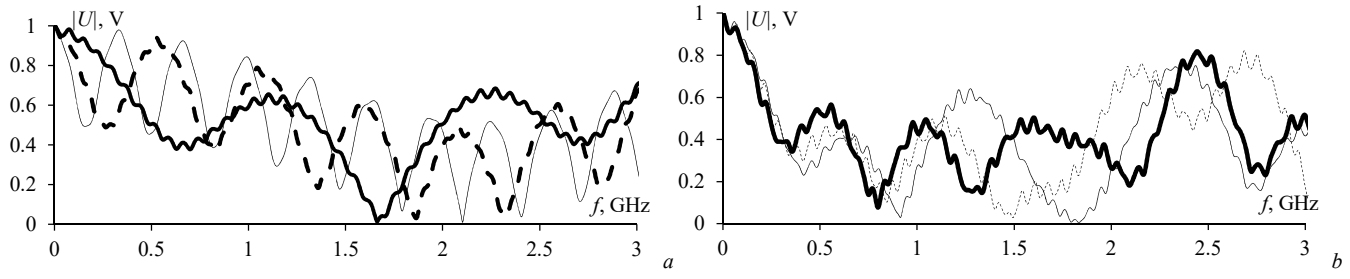

Fig. 6. Frequency responses of the MCTL with the reference conductor around (*a*) and above and below (*b*) at parameter sets 1 (——), 2 (—) and 3 (– –).

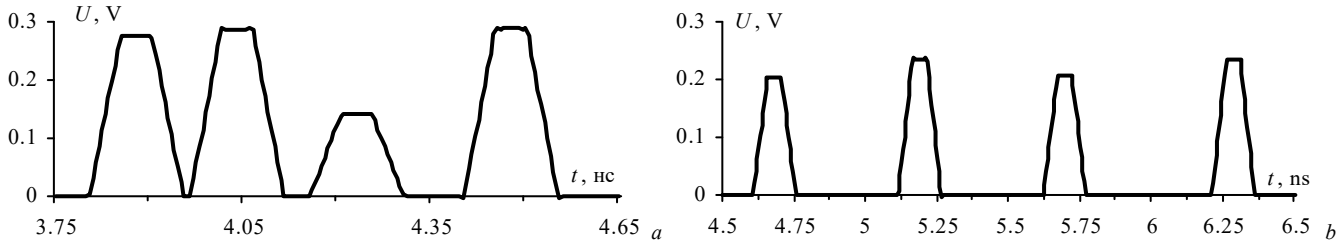

Fig. 7. Voltage waveforms at the MCTL output with the reference conductor around (*a*) and above and below (*b*) after optimization.

V. Conclusion

The analysis of the MCTLs with the reference conductor around and above and below for triple MR was performed. As a result, it was revealed that when the lines are simulated in the range of specified parameters, the deviations of the U_{max} values are insignificant, and the values of Δf and f_1 are almost the same only for the MCTL with the reference conductor above and below. Meanwhile, for this structure, there are deviations in the output signal shapes (in time and frequency responses). For the MCTL with the reference conductor around, there are deviations both in the waveforms of the output signal (in time and frequency responses) and in the values of Δf for different parameter sets. Thus, attenuation (relative to the input voltage) for the MCTL with the reference conductor around and above and below was achieved: for trapezoidal pulse – by 2.01 and 3.98 times; for ESD – by 1.9 A and 1.32 A, and for the pulse of a real USP generator – by 2.28 and 5.29 times, respectively. As a result of optimization by heuristic search, it was possible to increase the attenuation of the output voltage (from 0.5 V to 0.29 V and from 0.25 V to 0.24 V, respectively), as well as equalize the time intervals between the decomposition pulses for the MCTL with the reference conductor above and below.

Based on the obtained data, it can be concluded that both MCTLs can be successfully used for the implementation of new devices with triple MR (after additional parametric optimization), and the possibility of creating such MCTLs is justified by the reality of constructive and technological implementations.

References

[1] S. Vass, “Defense against electromagnetic pulse weapons,” Aarms, 2004, vol. 3, no. 3, pp. 443–457.

[2] Z.M. Gizatullin, R.M. Gizatullin, “Investigation of the immunity of computer equipment to the power-line electromagnetic interference,” Journal of Communications Technology and Electronics, no. 5, pp. 546–550, 2016.

[3] I. Bolvashenkov, J. Kammermann, H. Hans-Georg, “Methodology for quantitative assessment of fault tolerance of the multistate safety-critical systems with functional redundancy,” 2017 International Conference on Information and Digital Technologies (IDT), pp. 74–82, 2017.

[4] N. Mora, F. Vega, G. Lugrin, F. Rachidi, M. Rubinstein, “Study and classification of potential IEMI sources,” System and assessment notes, Note 41, 8 July, 2014.

[5] T. Weber, R. Krzikalla, J. L. Ter Haseborg, F. Sabath, “Linear and nonlinear filters suppressing,” IEEE Trans. Electromagn. Compat., no. 46, pp. 423–430, 2004.

[6] A.T. Gazizov, A.M. Zabolotsky, T.R. Gazizov, “UWB pulse decomposition in simple printed structures,” IEEE Transactions on Electromagnetic Compatibility, vol. 58, no. 4, pp. 1136–1142, 2016.

[7] T.R. Gazizov, P.E. Orlov, A.M. Zabolotskiy, E.N. Buichkin, “New method of routing of the printed conductors of redundant circuits,” Proceedings of TUSUR University, no. 3, pp. 129–131, 2015.

[8] A.V. Medvedev, V.R. Sharafutdinov, “Using modal reservation for ultrashort pulse attenuation after failure,” Proc. of IEEE 2019 International multi-conference on engineering, computer and information sciences (SIBIRCON), 2019, pp 1–4.

[9] A.V. Medvedev, T.R. Gazizov, Y.S. Zhechev, “Evaluating modal reservation efficiency before and after failure,” Journal of Physics: Conference Series, pp. 1–4, 2020.

[10] T.R. Gazizov, P.E. Orlov, V.R. Sharafutdinov, “A method for triple circuits reservation in multilayer printed circuit boards,” Russian Federation Patent 2663230 № 2017113045/07, Aug. 02, 2018.

[11] S.P. Kuksenko, “Preliminary results of TUSUR University project for design of spacecraft power distribution network: EMC simulation,” IOP Conf. Series: Materials Science and Engineering, vol. 560, no. 012110, pp. 1–7, 2019.

[12] A.O. Belousov, T.R. Gazizov, “Systematic approach to optimization for protection against intentional ultrashort pulses based on multiconductor modal filters,” Complexity, no. 2018, pp. 1–15, 2018.

[13] E.B. Chernikova, A.O. Belousov, T.R. Gazizov, A.M. Zabolotsky, “Using reflection symmetry to improve the protection of radio-electronic equipment from ultrashort pulses,” Symmetry, 2019, vol. 11(7), no. 883, pp. 1–25.